[Article] DOI: 10.13208/j.electrochem.2214007 Http://electrochem.xmu.edu.cn

The Rapid Preparation of Efficient MoFeCo-Based Bifunctional Electrocatalysts via Joule Heating for Overall Water Splitting

Ao Zhou, Wei-Jian Guo, Yue-Qing Wang*, Jin-Tao Zhang*
(*Key Laboratory for Colloid and Interface Chemistry Ministry of Education, School of Chemistry and Chemical Engineering, Shandong University, Jinan 250100, Shandong, China*)

Abstract: Water electrolysis is an available way to obtain green hydrogen. The development of highly efficient electrocatalysts is a current research hotspot for water splitting, but it remains challenging. Herein, we demonstrate the synthesis of a robust bifunctional multi-metal electrocatalysts toward water splitting via the rapid Joule-heating conversion of metal precursors. The composition and morphology were well regulated via altering the ratio of metal precursors. In particular, the trimetal MoC/FeO/CoO/carbon cloth (CC) electrode revealed the outstanding bifunctional electrocatalytic performance due to the unique composition and large electrochemical active surface area. Typically, the MoC/FeO/CoO/CC catalyst needed low overpotentials of 121 and 268 mV to reach 10 mA·cm^{-2} toward HER and OER in 1 mol·L^{-1} KOH solution, respectively. When used as both cathode and anode, a small potential of 1.69 V was required to achieve 10 mA·cm^{-2} for overall water splitting and an impressive stability for 25 h was observed. This facile and rapid Joule heating strategy offers guideline for rational manufacture of bimetal or multi-metal electrocatalysts toward diverse application.

Key words: hydrogen evolution reaction; oxygen evolution reaction; bifunctional electrocatalyst; water splitting; Joule heating

1 Introduction

Advanced energy has always been a necessary resource for human survival and social development, and the development of green and sustainable alternative energy has become the consensus with the increasing fossil energy issues[1, 2]. Hydrogen energy is a kind of clean secondary energy, which has the advantages of zero carbon emission, high calorific value and renewable energy. Electrocatalytic water splitting is a feasible way to generate hydrogen, aimed to solve global energy and environmental problems[3-8]. However, it is always suffered from the slow kinetics with the high cost, which greatly affects the promotion and application of water electrolysis technology[9-13]. At present, precious metal-based electrocatalysts are considered as the most efficient electrocatalysts toward water splitting, but the scarce and expensive price limit their potential application. Therefore, developing efficient non-precious metal-based electrocatalysts is pivotal[14-19].

Fabricating three-dimensional self-supported nanostructures not only avoids the use of non-conductive binders, but also provides a larger surface area to expose ample active sites, thus improving the catalytic activity[20-28]. For decades, bifunctional electrocatalysts being capable of performing both oxygen and hydrogen evolution reactions in the same electrolyte have attracted great attention due to the ability to enable practical applications of overall water splitting[29-33].

Cite as: Zhou A, Guo W J, Wang Y Q, Zhang J T. The rapid preparation of efficient MoFeCo-based bifunctional electrocatalysts via Joule heating for overall water splitting. *J. Electrochem.*, 2022, 28(9): 2214007.

Received: 2022-06-28, Revised: 2022-07-21. *Corresponding author, Tel: (86-531)88361011, E-mail: Jin-Tao Zhang, jtzhang@sdu.edu.cn; Yue-Qing Wang, Tel: (86-531)88361011, wangyueqing@sdu.edu.cn

For metal carbides, electrons are easily transferred from metal to carbon atoms, which raises the center of d-band and reduces the antibonding state between O atom intermediates to enhance the bonding strength of O atoms and improve the performance of OER[34]. Metal oxides have a large number of active sites and are beneficial to the adsorption and dissociation of H_2O, which is beneficial to improve the catalytic activity[35]. For the traditional material synthesis strategies including temperature programmed carbonization, carbothermic reduction and precipitation, such consumed processes may also cause the sintering and/or agglomeration issues. Significantly different from the aforementioned approaches, a series of new materials could be synthesized in a short time via Joule heating approach[36-38].

Herein, we demonstrated the fabrication of a bifunctional electrocatalyst via a Joule-heating treatment of diverse metal precursor on carbon fibers. With the preparations of bimetallic and polymetallic electrocatalysts via modifying the composition of metal precursors, the trimetallic MoC/FeO/CoO/CC demonstrated the excellent bifunctional electrocatalytic activity with 121 and 268 mV to deliver 10 $mA \cdot cm^{-2}$ for HER and OER, respectively. Furthermore, when the MoC/FeO/CoO/CC was used as an anode and a cathode for overall water splitting, only the potential of 1.69 V was required to reach 10 $mA \cdot cm^{-2}$, and the excellent stability was achieved. Reasonable design of robust and efficient non-noble metal electrocatalysts is of great significance for promoting the commercialization of water electrolysis for hydrogen production.

2 Experimental Section

2.1 Synthesis of MoC/FeO/CoO/CC

The carbon cloth (CC) was activated via immersing in nitric acid at 90 °C for 10 hours and then ultrasonic cleaning in deionized water for several times [39]. 0.05 mol $C_{10}H_{14}MoO_6$, 0.05 mol $C_{15}H_{21}FeO_6$ and 0.05 mol $Co(C_5H_7O_2)_2 \cdot xH_2O$ were completely dissolved in 10 mL of N, N-Dimethylformamide. Then, 1.4 mL of the mixed solution was dropped on a piece of CC (1 × 7 cm). After being dried at 30 ℃, the metal precursor coated CC was heated to 1000 ℃ in a vacuum environment via Joule-heating, and finally, the electrocatalyst was obtained and is named as Mo_2C/Fe_3O_4/CoO. Followed the similar procedure, diverse bimetal electrodes were prepared and are named as MoC/FeO/CC, MoC/CoO/MoO/CC, and FeO/CoO/CC via employing two metal precursors. Similarity, the trimetal catalysts $Mo_{0.5}C$/FeO/CoO/CC and Mo_2C/FeO/CoO/CC were also synthesized via altering the ratio of different metal precursors.

2.2 Material Characterizations

The microstructure and morphology of electrocatalysts were characterized by field emission scanning electron microscope (FESEM, Zeiss, Sigma 300), transmission electron microscope (TEM, JEM-2100F) and the high-angle annular dark-field scanning TEM (HAADF-STEM, JEOL JEM-ARM300F). The crystalline structure was analyzed on X-ray diffractometer (Bruker D8 diffractometer) with Cu K_α radiation (λ = 0.15418 nm). The X-ray photoelectron spectro scopic (XPS) analysis was carried out with a multipurpose X-ray photoemission spectroscope (Thermo Scientific ESCALAB 250Xi).

2.3 Electrochemical Measurements

The electrochemical measurements in a typical three-electrode system where a graphite rod served as the counter electrode, a Ag/AgCl electrode as the reference electrode and the as-synthesized electrode as the working electrode in 1.0 $mol \cdot L^{-1}$ KOH. All the potential data tested were converted to reversible hydrogen electrode (RHE) scales by the equation (1)[23, 40]:

$$E_{RHE} = 0.197 + 0.059pH + E_{Ag/AgCl} \quad (1)$$

Linear sweep voltammetry (LSV) was used to evaluate the electrocatalytic activity by measuring LSV curves at 5 $mV \cdot s^{-1}$ with 95% *iR* compensation. Electrochemical impedance spectroscopic (EIS) test was performed with 5 mV AC amplitude in the frequency range from 100 KHz to 0.01 Hz and the applied potentials were -0.18 and 1.52 V for HER and OER, respectively. The cyclic voltammetric (CV) curves were recorded in a non-Faradaic region of 0.12 ~ 0.22 V for HER and 1.22 ~ 1.32 V for OER at different scan rates from 20 to 100 $mV \cdot s^{-1}$. And the value of double-

layer capacitance (C_{dl}) was used to reflect the electrochemically active surface area (ECSA). The ECSA value was calculated by the using ECSA = C_{dl}/C_s, where C_s is the specific capacitance, and C_s = 0.040 mF·cm^{-2} in 1 mol·L^{-1} KOH solution[41, 42]. To assess the overall water splitting performance, the MoC/FeO/CoO/CC electrodes were employed as both anode and cathode. Faraday efficiency was obtained by the volumes of hydrogen and oxygen produced in a certain period of time.

3 Results and Discussion

With the coating of metal precursors on CC, the Joule-heating treatment enables the rapid surface conversion due to the carbon thermal reaction (Schemed in Figure 1). Thus, diverse bimetal- or multi-metal-based electrocatalysts were directly grown on CC via altering the precursor ratio.

As revealed in SEM images, the irregular nanosheets for MoC/FeO/CoO/CC were formed and distributed on the whole surface of CC (Figure 2a-c).

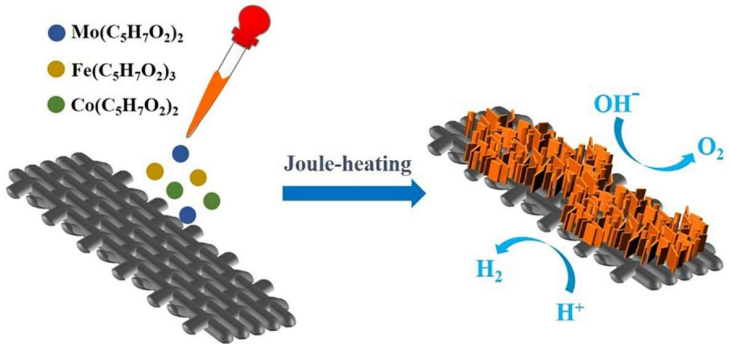

Figure 1 Schematic illustration for the synthesis of metal-based electrocatalysts on CC via one-step Joule heating (color on line)

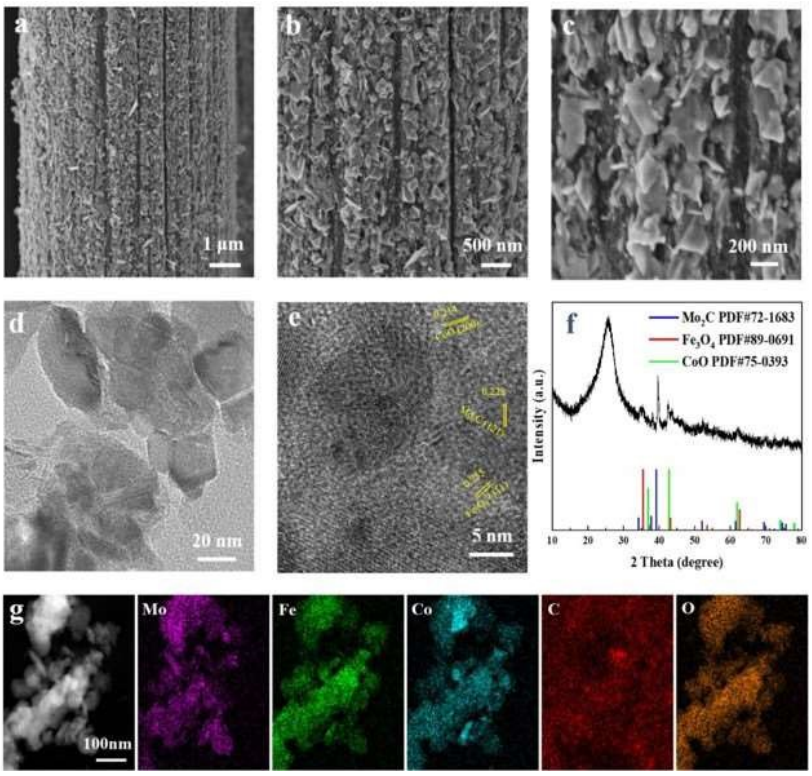

Figure 2 (a-c) SEM, (d) TEM and (e) HRTEM images, (f) XRD pattern and (g) the corresponding element mapping images of MoC/FeO/CoO/CC. (color on line)

However, lots of nanoparticles were deposited on the carbon fiber surface for MoC/FeO/CC and FeO/CoO/CC samples, and the agglomeration phenomenon of MoC/CoO/MoO/CC was obvious (Figure S1). The crystal structure of MoC/FeO/CoO/CC was analyzed by XRD (Figure 2f), the diffraction peaks of MoC/FeO/CoO/CC were indexed to Mo_2C, Fe_3O_4, and CoO, respectively, suggesting the formation of hybrid structure. Mo_2C is a promising catalyst for hydrogen evolution due to its inherent metallicity and high stability, and the abundant heterointerfaces synergistically promote the performance of water electrolysis[43,44]. The TEM images (Figure 2d-e) reveal that the lattice spacings of 0.228, 0.255, and 0.214 nm corresponded to the crystal planes of Mo_2C (121), Fe_3O_4 (311), and CoO (200), respectively, indicating the formation of heterostructures. The corresponding element mapping images further confirm that the elements of Mo, Fe, Co, C, O were uniformly distributed (Figure 2g).

XPS data was also analyzed in order to further disclose the surface valence state (Figure 3). In the high-resolution Mo 3d spectrum of MoC/FeO/CoO/CC (Figure 3a), the two peaks situated at 229.9 and 232.2 eV are belonging to the Mo $3d_{5/2}$ and Mo $3d_{3/2}$ of Mo^{2+}, indicating the formation of Mo_2C[45]. The peaks located at 230.8 and 234.0 eV are assigned to MO^{4+} and Mo^{6+}, respectively, which would be contributed to the exist of Mo oxide on the surface of MoC/FeO/CoO/CC due to surface oxidation[46]. For Fe 2p spectrum (Figure 3b), two major peaks of Fe^{3+} located at 715.4 and 727.6 eV, and 711.7 and 724.5 eV are assigned to

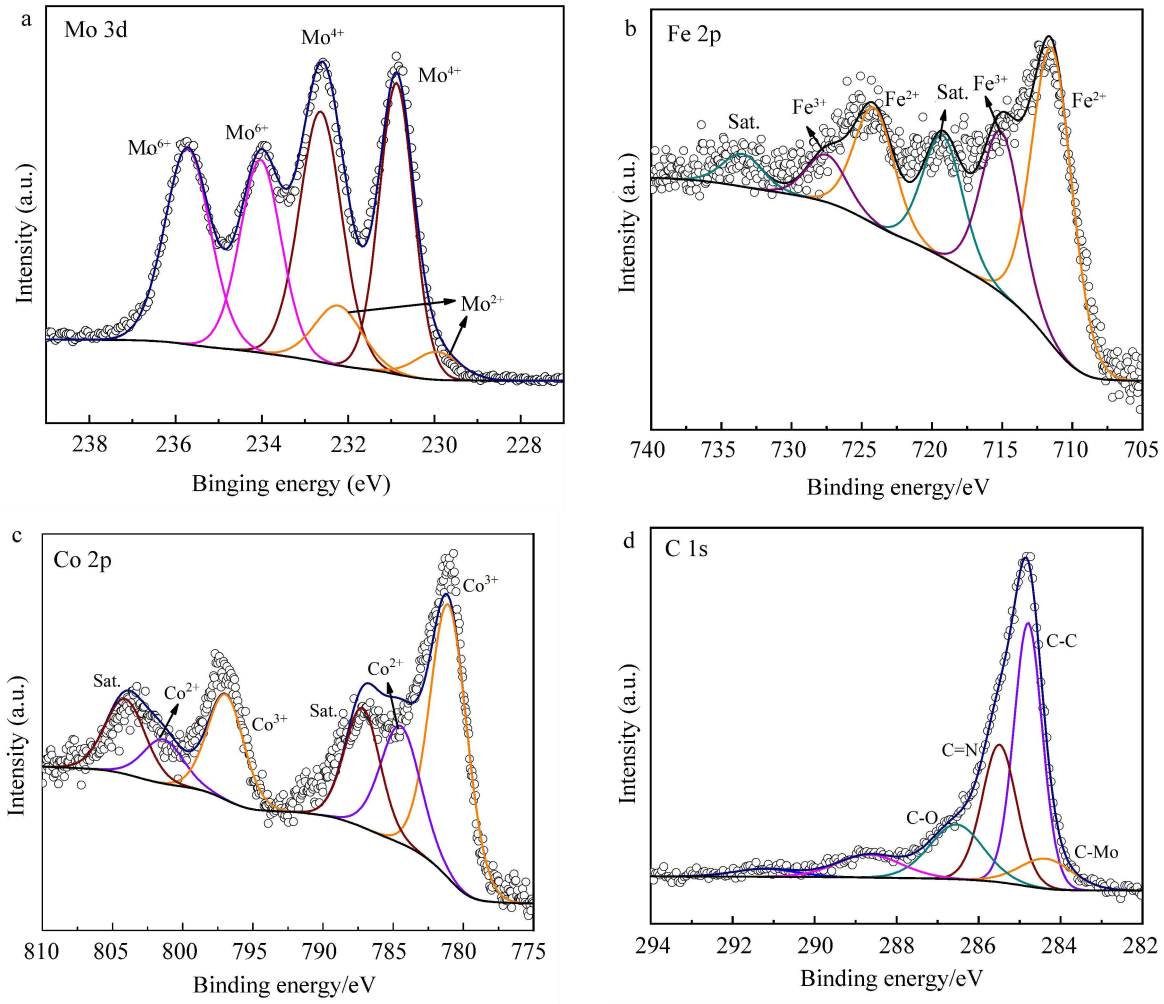

Figure 3 High-resolution XPS spectra of (a) Mo 3d, (b) Fe 2p, (c) Co 2p, and (d) C 1s of MoC/FeO/CoO/CC. (color on line)

Fe^{2+}[1, 47, 48]. Additionally, Co 2p XPS spectrum (Figure 3c) reveal the binding energies for Co^{3+} (784.7 and 801.3 eV) and Co^{2+} (781.2 and 797.0 eV)[5,46]. Figure S3 shows the two O 1s peaks of MoC/FeO/CoO/CC at 530.8 and 531.6 eV. The binding energy at 284.4 eV attributed to C-Mo bond in the deconvoluted C 1s spectrum (Figure 3d), further illustrated the formation of metal carbide[49, 50]. All those results demonstrate that the formation of carbide and oxides heterostructures via the rapid Joule heating strategy (Figure S2).

In order to evaluate the HER performance, the electrochemical properties were tested in 1.0 mol·L^{-1} KOH solution. As shown in Figure 4a, the MoC/FeO/CoO/CC electrode reveals superb hydrogen evolution catalytic performance, only 121 mV to reach 10 mA·cm^{-2}. This value is prominently lower than those of MoC/FeO/CC (174 mV), MoC/CoO/MoO/CC (214 mV), and FeO/CoO/CC (234 mV), indicating that the formation of triphase metal carbide and oxide heterostructures is beneficial to the boosted HER performance. In addition, the HER performance could be well regulated via altering the precursor ratio. The $Mo_{0.5}C$/FeO/CoO/CC and Mo_2C/FeO/CoO/CC electrodes exhibited the inferior HER performance in comparison with the MoC/FeO/CoO/CC (Figure S4), and the high overpotentials of 139 and 152 mV were required, indicating rational regulation of the composition could contribute to the optimized HER performance. Tafel slope is a typical descriptor, reflecting the reaction kinetics characters. The MoC/FeO/CoO/

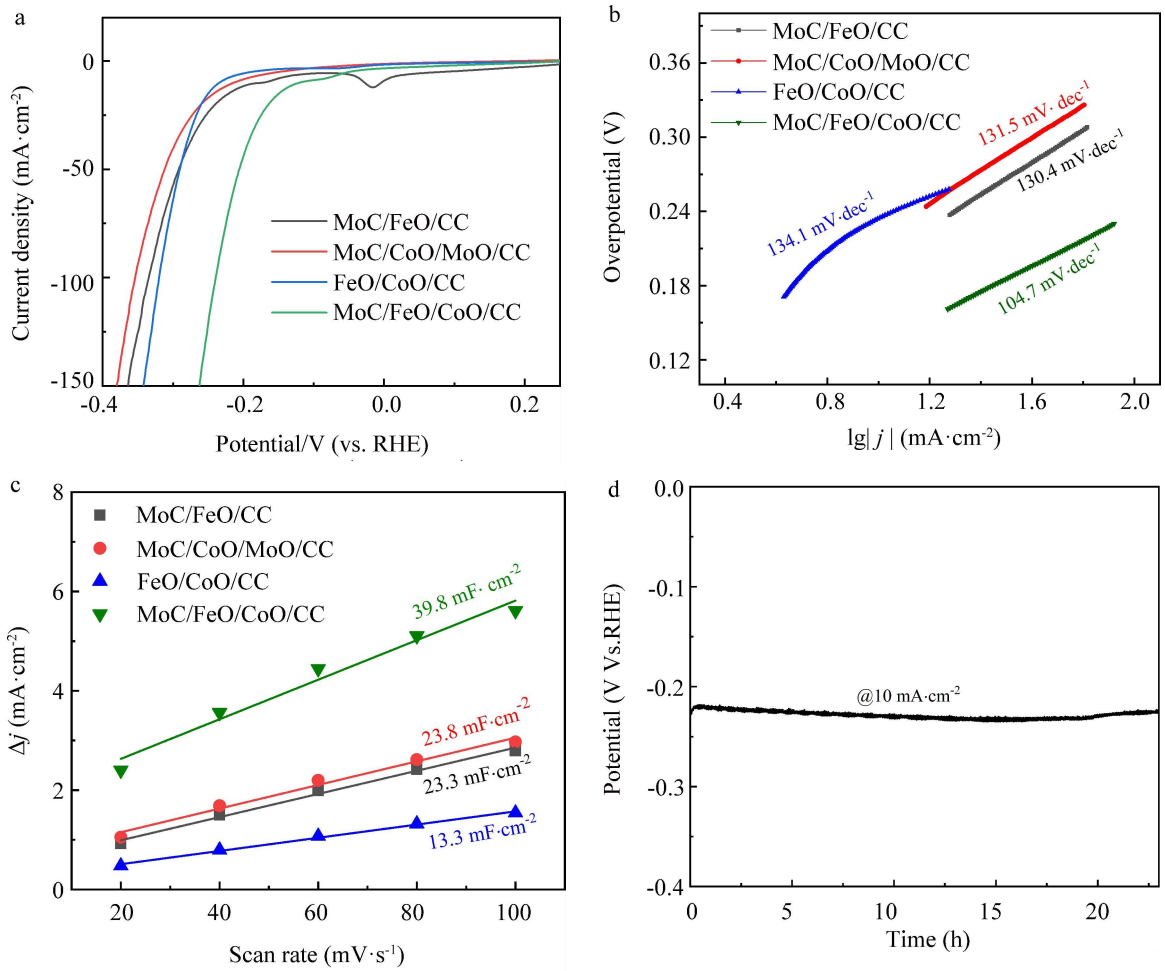

Figure 4 HER performances of diverse electrocatalysts. (a) Linear sweep voltammetric polarization curves, (b) the corresponding Tafel slopes, and (c) plots of the current density at different scan rates. (d) Chronopotentiometric curve of MoC/FeO/CoO/CC at 10 mA·cm^{-2}. (color on line)

CC electrode demonstrated the smallest Tafel slope of 104.7 mV·dec^{-1}, significantly lower than the bimetal electrocatalysts including MoC/FeO/CC (130.4 mV·dec^{-1}), MoC/CoO/MoO/CC (131.5 mV·dec^{-1}), FeO/CoO/CC (134.1 mV·dec^{-1}), and trimetal electrocatalysts like $Mo_{0.5}C$/FeO/CoO/CC (122.3 mV·dec^{-1}) and Mo_2C/FeO/CoO/CC (109.0 mV·dec^{-1}), suggesting the much easier reaction kinetics of MoFeCo heterostructure (Figures 4b and S5). To further explore the excellent electrocatalytic performance, the double-layer capacitance (C_{dl}) was calculated (Figures 4c and S6). ECSA is proportional to C_{dl}, hence, a higher C_{dl} value indicates a larger electrochemical active surface. The C_{dl} value of MoC/FeO/CoO/CC was 39.8 mF·cm^{-2}, which is significantly higher than those of the bimetal- and tri-metal-based electrocatalysts (Figure S7). The MoC/FeO/CoO/CC showed a high active area, suggesting ample exposed active sites number, which contributes to excellent HER performance. Impedance is composed of real and imaginary parts, resistance is represented by real part, while reactance and capacitance are represented by positive and negative imaginary parts, respectively. Electrochemical impedance spectroscopic (EIS) data demonstrates the similar semicircular nearly identical origins (Figure S8). It was obviously that the charge transfer resistance of MoC/FeO/CoO/CC (5.62 Ω) was smaller than those of other samples, facilitating electron transfer at the electrolyte/electrode interface (Table S1). During the stability test period, the voltage of MoC/FeO/CoO/CC showed a negligible change, demonstrating the fantastically stable electrochemical

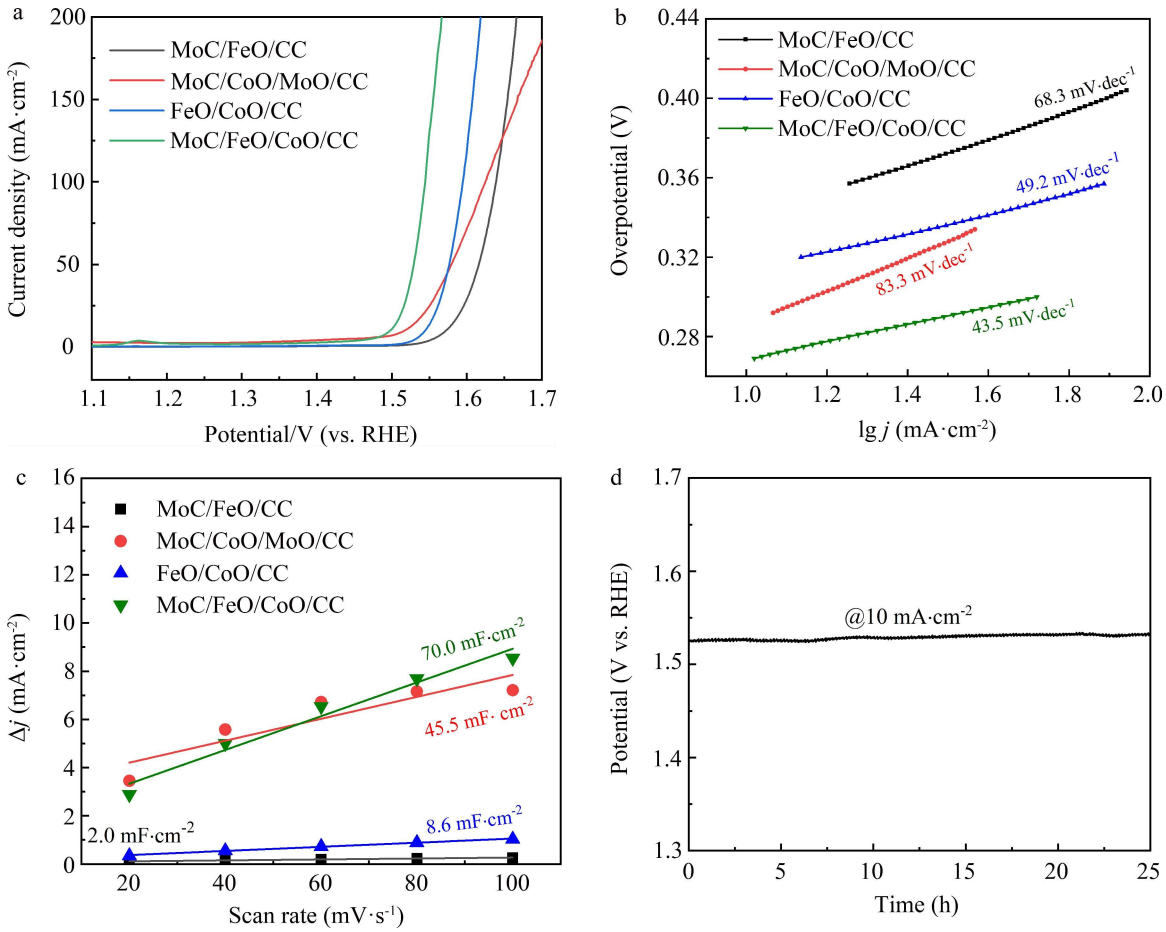

Figure 5 OER performances of different catalysts in 1.0 mol·L^{-1} KOH solution. (a) Linear sweep voltammetric polarization curves, (b) Corresponding Tafel slopes, (c) Plots of the current density at different scan rates, (d) Chronopotentiometric curve of MoC/FeO/CoO/CC at 10 mA·cm^{-2}. (color on line)

performance of MoC/FeO/CoO/CC due to synergy between multiple components (Figure 4d).

The OER performance was further appraised in KOH. As shown in Figure 5a, the MoC/FeO/CoO/CC electrode demonstrated superior oxygen evolution catalytic activity with a low overpotential of 268 mV to achieve 10 mA·cm^{-2}. This value is significantly lower than those of MoC/FeO/CC (342 mV), MoC/CoO/MoO/CC (287 mV), and FeO/CoO/CC (314 mV), indicating the synergy between metal carbide and oxide heterostructures contributed to the OER performance. It was also lower than those of $Mo_{0.5}C$/FeO/CoO/CC (281 mV) and Mo_2C/FeO/CoO/CC (278 mV) (Figure S9), suggesting that optimizing the content of Mo is beneficial to OER performance. The MoC/FeO/CoO/CC electrode revealed a smaller Tafel slope of 43.5 mV·dec^{-1} (Figure 5b, S10), which is lower than these of bimetal or trimetal electrocatalysts. The smallest Tafel slope indicates that the MoC/FeO/CoO/CC sample owns the rapid reaction kinetic process. The largest C_{dl} value of 70.0 mF·cm^{-2} for MoC/FeO/CoO/CC catalyst (Figure 5c, S11-12) indicates the larger electrochemical active surface for ample active sites exposure. The smaller the radius of the circle, the faster the rate of charge transfer. The MoC/FeO/CoO/CC electrode had the smallest R_{ct} value of 2.41 Ω, which is distinctly lower than that of MoC/FeO/CC (3.07 Ω), MoC/CoO/MoO/CC (11.58 Ω), and FeO/CoO/CC (3.05 Ω) electrodes (Figure S13, Table S2), indicating a faster charge transfer capa-

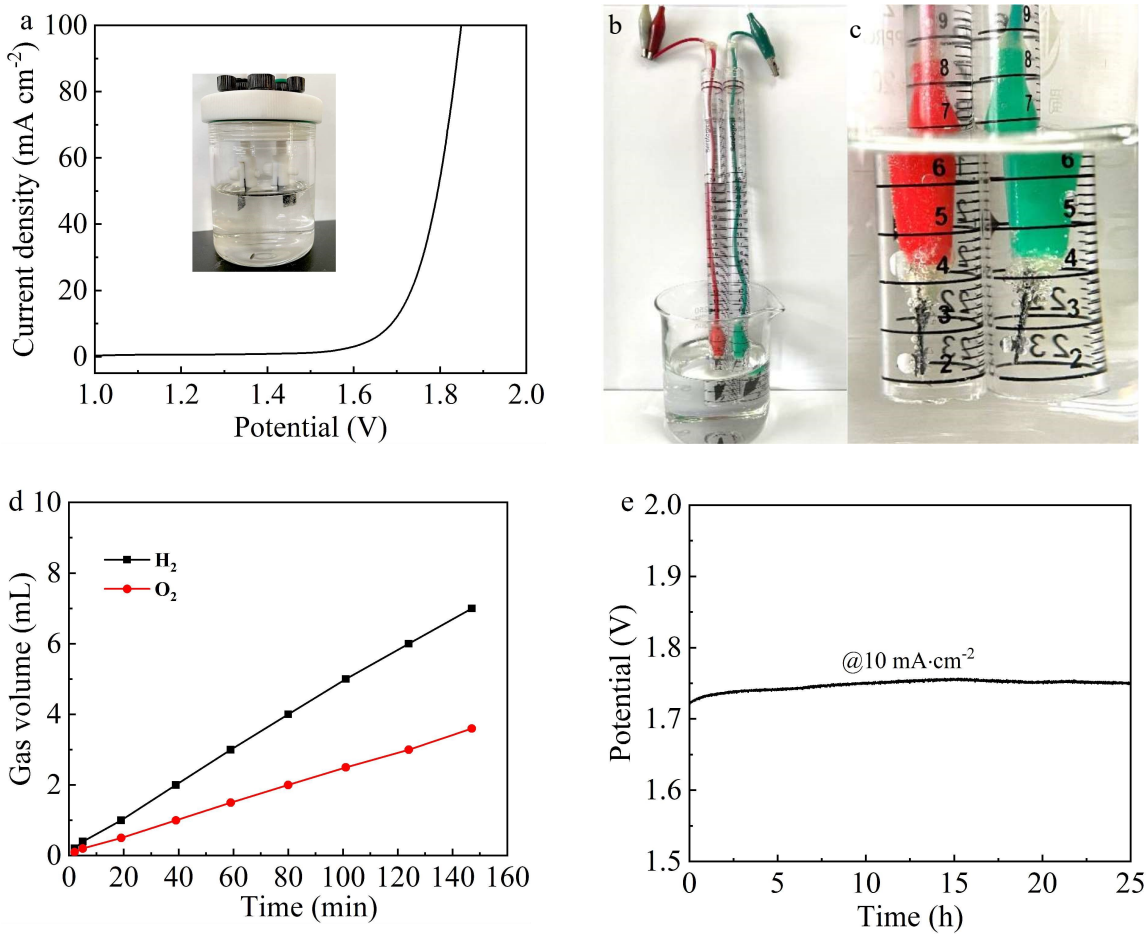

Figure 6 Overall water splitting performance. (a) Polarization curve of MoC/FeO/CoO/CC (+) || MoC/FeO/CoO/CC (–) in 1 mol·L^{-1} KOH solution. (b, c) Photographs of the apparatus used for overall water splitting for testing the volumes of gas generated by a drainage method. (d) The amount of gas produced at different time at 8 mA·cm^{-2}. (e) Chronopotentiometric curve at 10 mA·cm^{-2}. (color on line)

bility among these samples. Formations of trimetallic nanosheets and hybrid structures significantly reduced the charge transfer resistance. The stability of MoC/FeO/CoO/CC was evaluated by chronopotentiometric measurement at 10 mA·cm^{-2}, and the potential remained stable during the test period, indicating that rich interfaces can expose plenty of active sites (Figure 5d). The large surface area, ample heterogeneous interface and mechanical stability synergy would achieve its superb catalytic activity and long-term stability.

Encouraged by the excellent OER and HER performances, overall water splitting performance was tested in a two-electrode system with the MoC/FeO/CoO/CC electrode as both anode and cathode (Figure 6a). The onset potential of the MoC/FeO/CoO/CC (+) || MoC/FeO/CoO/CC (−) electrodes was about 1.5 V. And the MoC/FeO/CoO/CC (+) || MoC/FeO/CoO/CC (−) electrodes required a potential of 1.69 V to reach 10 mA·cm^{-2} for overall water splitting. To detect the rate of gas production during the water splitting process, a home-made device (Figure 6b-c) was designed, in which two identical MoC/FeO/CoO/CC electrodes were immersed in a sealed graduated pipette. The H_2 and O_2 produced could be quantitatively recorded through the drainage strategy. A good linear relationship between the electrolytic time and the gas productions of H_2 and O_2 was observed (Figure 6d). The volume ratio of hydrogen to oxygen produced during the test time is about 2:1, which matched well with the theoretical value. The result indicated that the Faraday efficiencies of MoC/FeO/CoO/CC catalyst toward HER and OER were 93.1% and 95.7%, respectively. The chronopotentiometric curve reveals the potential drop for only 40 mV during 25-h electrolysis, which further proves the outstanding stability (Figure 6e). Therefore, the excellent electrocatalytic performance of MoC/FeO/CoO/CC catalyst for overall water splitting indicates that the MoC/FeO/CoO/CC exhibited fantastic activity and stability as a new type of bifunctional electrocatalyst in practical applications.

4 Conclusions

In summary, we demonstrated the rapid synthesis of three-dimensional metal carbide and oxide heterogeneous structures via Joule heating strategy. Upon altering the precursor composition, the structure and composition were well regulated, which enables the synthesis of diverse bimetal and trimetal heterogeneous structures. Typically, the resultant MoC/FeO/CoO/CC catalyst revealed the excellent bifunctional catalytic performance with the overpotentials of 121 and 268 mV to deliver 10 mA·cm^{-2} for HER and OER, respectively. When employed as both anode and cathode for overall water splitting, only 1.69 V was required to achieve 10 mA·cm^{-2}. These approaches and understanding will provide a new way for rational design and exploration of sustainable and dual-function electrocatalysts for low-cost and environmentally friendly industrial hydrogen production.

Acknowledgements:

Authors gratefully acknowledge the financial supports from the National Natural Science Foundation of China (No. 22175108) and the Natural Scientific Foundation (No. ZR2020JQ09).

References:

[1] Cai S H, Chen X N, Huang M J, Han J Y, Zhou Y W, Li J S. Interfacial engineering of nickel/iron/ruthenium phosphides for efficient overall water splitting powered by solar energy[J]. J. Mater. Chem. A., 2022, 10(2): 772-778.

[2] Chang J F, Wang G Z, Yang Z Z, Li B Y, Wang Q, Kuliiev R, Orlovskaya N, Gu M, Du Y G, Wang G F, Yang Y. Dual-doping and synergism toward high-performance seawater electrolysis[J]. Adv. Mater., 2021, 33(33): 2101425.

[3] Wang Y Q, Ma J Z, Wang J, Chen S, Wang H S, Zhang J T. Interfacial scaffolding preparation of hierarchical PBA-based derivative electrocatalysts for efficient water splitting[J]. Adv. Energy Mater., 2019, 9(5): 1802939.

[4] Wang Y Q, Zhang B H, Pan W, Ma H Y, Zhang J T. 3 D porous nickel-cobalt nitrides supported on nickel foam as efficient electrocatalysts for overall water splitting[J]. ChemSusChem, 2017, 10(21): 4170-4177.

[5] Gautam J, Liu Y, Gu J, Ma Z Y, Zha J J, Dahal B, Zhang L N, Chishti A N, Ni L B, Diao G W, Wei Y G. Fabrication of polyoxometalate anchored zinc cobalt sulfide nanowires as a remarkable bifunctional electrocatalyst for

overall water splitting[J]. Adv. Funct. Mater., 2021, 31(46): 2106147.

[6] Gu M Z, Deng X Y, Lin M, Wang H, Gao A, Huang X M, Zhang X J. Ultrathin NiCo bimetallic molybdate nanosheets coated CuO_x nanotubes: Heterostructure and bimetallic synergistic optimization of the active site for highly efficient overall water splitting[J]. Adv. Energy Mater., 2021, 11(41): 2102361.

[7] Kim Y, Kim D, Lee J, Lee L. Tuning the electrochemical properties of polymeric cobalt phthalocyanines for efficient water splitting[J]. Adv. Funct. Mater., 2021, 31(41): 2103290.

[8] Yang H, Liu Y F, Liu X L, Wang X K, Tian H, Waterhouse G, Kruger P, Telfer S, Ma S Q. Large-scale synthesis of N-doped carbon capsules supporting atomically dispersed iron for efficient oxygen reduction reaction electrocatalysis[J]. eScience, 2022, 2: 227-234.

[9] Li S S, Wang L, Su H, Hong A N, Wang Y X, Yang H J, Ge L, Song W Y, Liu J, Ma T Y, Bu X H, Feng P Y. Electron redistributed S-doped nickel iron phosphides derived from one-step phosphatization of MOFs for significantly boosting electrochemical water splitting[J]. Adv. Funct. Mater., 2022, 32(23): 2200733.

[10] Li W, Liu J, Guo P F, Li H Z, Fei B, Guo Y H, Pan H G, Sun D L, Fang F, Wu R B. Co/CoP heterojunction on hierarchically ordered porous carbon as a highly efficient electrocatalyst for hydrogen and oxygen evolution [J]. Adv. Energy Mater., 2021, 11(42): 2102134.

[11] Lin Z P, Xiao B B, Wang Z P, Tao W Y, Shen S J, Huang L A, Zhang J T, Meng F Q, Zhang Q H, Gu L, Zhong W W. Planar-coordination $PdSe_2$ nanosheets as highly active electrocatalyst for hydrogen evolution reaction[J]. Adv. Funct. Mater., 2021, 31(32): 2102321.

[12] Liu C, Qian J, Ye Y F, Zhou H, Sun C J, Sheehan C, Zhang Z Y, Wan G, Liu Y S, Guo J H, Li S, Shin H, Hwang S, Gunnoe T B, Goddard W A, Zhang S. Oxygen evolution reaction over catalytic single-site Co in a well-defined brookite TiO_2 nanorod surface[J]. Nat. Catal., 2021, 4(1): 36-45.

[13] Liu H X, Li X Y, Chen L L, Zhu X D, Dong P, Chee M, Ye M X, Guo Y H, Shen J F. Monolithic Ni-Mo-B bifunctional electrode for large current water splitting [J]. Adv. Funct. Mater., 2022, 32(4): 2107308.

[14] Li Y, Jiang K Y, Yang J, Zheng Y Y, Hubner R, Ou Z W, Dong X, He L Q, Wang H L, Li J, Sun Y J, Lu X B, Zhuang X D, Zheng Z K, Liu W. Tungsten oxide/reduced graphene oxide aerogel with low-content platinum as high-performance electrocatalyst for hydrogen evolution reaction[J]. Small, 2021, 17(37): 2102159.

[15] Peng Y, Liu Q M, Lu B Z, He T, Nichols F, Hu X, Huang T, Huang G, Guzman L, Ping Y, Chen S W. Organically capped iridium nanoparticles as high-performance bifunctional electrocatalysts for full water splitting in both acidic and alkaline media: Impacts of metal-ligand interfacial interactions[J]. ACS Catal., 2021, 11(3): 1179-1188.

[16] Shan J Q, Ye C, Chen S M, Sun T L, Jiao Y, Liu L M, Zhu C Z, Song L, Han Y, Jaroniec M, Zhu Y H, Zheng Y, Qiao S Z. Short-range ordered iridium single atoms integrated into cobalt oxide spinel structure for highly efficient electrocatalytic water oxidation[J]. J. Am. Chem. Soc., 2021, 143(13): 5201-5211.

[17] Wang H M, Chen Z N, Wu D S, Cao M N, Sun F F, Zhang H, You H H, Zhuang W, Cao R. Significantly enhanced overall water splitting performance by partial oxidation of Ir through Au modification in core-shell alloy structure[J]. J. Am. Chem. Soc., 2021, 143(12): 4639-4645.

[18] Wang M J, Xu Y, Peng C K, Chen S Y, Lin Y G, Hu Z W, Sun L, Ding S Y, Pao C W, Shao Q, Huang X Q. Site-specified two-dimensional heterojunction of Pt nanoparticles/metal-organic frameworks for enhanced hydrogen evolution[J]. J. Am. Chem. Soc., 2021, 143(40): 16512-16518.

[19] Wang T X, Guo L L, Jiang Z, Chen S T, Xu S R, Zhang Y X, Zhang J, Li R J, Peng T Y. Ru-Pincer complex-bridged Cu-porphyrin polymer for robust (photo) electrocatalytic H_2 evolution via single-atom active sites [J]. Adv. Funct. Mater., 2021, 31(50): 2107290.

[20] Wang X D, Wang C, Lai F Y, Sun H X, Yu N, Geng B Y. Self-supported CoFe-P nanosheets as a bifunctional catalyst for overall water splitting[J]. ACS Appl. Nano Mater., 2021, 4(11): 12083-12090.

[21] Zhang Q, Xiao W, Guo W H, Yang Y X, Lei J L, Luo H Q, Li N B. Macroporous array induced multiscale modulation at the surface/interface of $Co(OH)_2$/NiMo self-supporting electrode for effective overall water splitting [J]. Adv. Funct. Mater., 2021, 31(33): 2102117.

[22] Liu J C, Wang Y, Liao Y F, Wu C L, Yan Y G, Xie H J, Chen Y G. Heterostructured Ni_3S_2-Ni_3P/NF as a bifunctional catalyst for overall urea-water electrolysis for hydrogen generation[J]. ACS Appl. Mater. Interfaces., 2021, 13(23): 26948-26959.

[23] Riyajuddin S, Azmi K, Pahuja M, Kumar S, Maruyama T, Bera C, Ghosh K. Super-Hydrophilic hierarchical Ni-foam-graphene-carbon nanotubes-Ni_2P-CuP_2 nano-architecture as efficient electrocatalyst for overall water

splitting[J]. ACS Nano., 2021, 15(3): 5586-5599.

[24] Tang Y J, Zou Y, Zhu D D. Efficient water oxidation using an Fe-doped nickel telluride-nickel phosphide electrocatalyst by partial phosphating[J]. J. Mater. Chem. A., 2022.

[25] Wang X Y, Xie Y, Zhou W, Wang X W, Cai Z C, Xing Z P, Li M X, Pan K. The self-supported Zn-doped CoNiP microsphere/thorn hierarchical structures as efficient bifunctional catalysts for water splitting[J]. Electrochim. Acta., 2020, 339: 135933.

[26] Zhang B, Shan J W, Wang W L, Tsiakaras P, Li Y Y. Oxygen vacancy and core-shell heterojunction engineering of anemone-like CoP@CoOOH bifunctional electrocatalyst for efficient overall water splitting[J]. Small, 2022, 18(12): 2106012.

[27] Zhang B, Zheng Y J, Ma T, Yang C D, Peng Y F, Zhou Z H, Zhou M, Li S, Wang Y H, Cheng C. Designing MOF nanoarchitectures for electrochemical water splitting[J]. Adv. Mater., 2021, 33(17): 2006042.

[28] Lv Z, Ma W S, Wang M, Dang J, Jian K L, Liu D, Huang D J. Co-constructing interfaces of multiheterostructure on Mxene ($Ti_3C_2T_x$)-modified 3*d* self-supporting electrode for ultraefficient electrocatalytic HER in alkaline media[J]. Adv. Funct. Mater., 2021, 31(29): 2102576.

[29] Chen Y, Liu Q, Yao Y, Wu H B, Wang Y X, Zheng H Q, Cui Y J, Qian G D. Engineering different reaction centers on hierarchical Ni/NiFe layered double hydroxide accelerating overall water splitting[J]. ACS Appl. Energy Mater., 2021, 4(9): 9858-9865.

[30] Dai Z F, Geng H B, Wang J, Luo Y B, Li B, Zong Y, Yang J, Guo Y Y, Zheng Y, Wang X, Yan Q Y. Hexagonal-phase cobalt monophosphosulfide for highly efficient overall water splitting[J]. ACS Nano, 2017, 11(11): 11031-11040.

[31] Wang X, Zhang L, Liu C P, Ge J J, Zhu J B, Xing W. Recent advances in structural regulation on non-precious metal catalysts for oxygen reduction reaction in alkaline electrolytes[J]. J. Electrochem., 2022, 28(2): 2108501.

[32] Jiang X, Xie Q F, Lu G X, Wang Y, Liu T F, Liu Y J, Tao X Y, Nai J W. Synthesis of $NiSe_2/Fe_3O_4$ nanotubes with heteroepitaxy configuration as a high-efficient oxygen evolution electrocatalyst[J]. Small Methods, 2022: 2200377.

[33] Li L, Guo Y, Wang X R, Liu X W, Lu Y W. Ultraeven Mo-doped CoP nanocrystals as bifunctional electrocatalyst for efficient overall water splitting[J]. Langmuir, 2021, 37(19): 5986-5992.

[34] Chen Q W, Chen S, Zhao L L, Ma J Z, Wang H S, Zhang J T. Interface coating of iron nitride on carbon cloth for reversible lithium redox in rechargeable battery[J]. Chem. Eng. J., 2022, 431 (1), 133961.

[35] Cao X Y, Tan D X, Wulan B R, Zhang J T. *In situ* characterization for boosting electrocatalytic carbon dioxide reduction[J]. Small Methods, 2021, 5(10): 2100700.

[36] Chen Y N, Egan G C, Wan J Y, Zhu S Z, Jacob R J, Zhou W B, Dai J Q, Wang Y B, Danner V A, Yao Y G, Fu K, Wang Y B, Bao W Z, Li T, Zachariah M R, Hu L B. Ultra-fast self-assembly and stabilization of reactive nanoparticles in reduced graphene oxide films[J]. Nat. Commun., 2016, 7(1): 1-9.

[37] Yao Y G, Huang Z N, Xie P F, Lacey S D, Jacob R J, Xie H, Chen F J, Nie A, Pu T C, Rehwoldt M, Yu D W, Zachariah M, Wang C, Li J, Hu L B. Carbothermal shock synthesis of high-entropy-alloy nanoparticles[J]. Science, 2018, 359(6383): 1489-1494.

[38] Wu H, Lu Q, Zhang J F, Wang J J, Han X P, Zhao N Q, Hu W B, Li J J, Chen Y N, Deng Y D. Thermal shock-activated spontaneous growing of nanosheets for overall water splitting[J]. Nanomicro Lett., 2020, 12(1): 1-12.

[39] Chen P Z, Xu K, Fang Z W, Tong Y, Wu J C, Lu X L, Peng X, Ding H, Wu C Z, Xie Y. Metallic Co_4N porous nanowire arrays activated by surface oxidation as electrocatalysts for the oxygen evolution reaction[J]. Angew. Chem. Int. Ed., 2015, 54(49): 14710-14714.

[40] Dai Z F, Geng H B, Wang J, Luo Y B, Li B, Zong Y, Yang J, Guo Y Y, Zheng Y, Wang X, Yan Q Y. Hexagonal-phase cobalt monophosphosulfide for highly efficient overall water splitting[J]. ACS Nano, 2017, 11(11): 11031-11040.

[41] Wang P C, Liu X F, Yan Y T, Cao J, Feng J C, Qi J L. Exploring CoP core-shell nanosheets by Fe and Zn dual cation doping as efficient electrocatalysts for overall water splitting[J]. Catal. Sci. Technol., 2020, 10(5): 1395-1400.

[42] Liu T, Li P, Yao N, Cheng G Z, Chen S L, Luo W, Yin Y D. CoP-doped MOF-based electrocatalyst for pH-universal hydrogen evolution reaction[J]. Angew. Chem. Int. Ed., 58 (14): 4679-4684.

[43] Lou H, Yu T, Ma J N, Zhang S T, Bergara A, Yang G C. Achieving high hydrogen evolution reaction activity of a Mo_2C monolayer[J]. Phys. Chem. Chem. Phys., 2020, 22: 26189-26199.

[44] Zhang L Y, Zheng Y J, Wang J C, Geng Y, Zhang B, He J J, Xue J M, Frauenheim T, Li M. Ni/Mo bimetallic-oxide-derived heterointerface-rich sulfide nanosheets with Co-doping for efficient alkaline hydrogen evolution by boosting volmer reaction[J]. Small, 2021, 17(10): 2006730.

[45] Wan J, Wu J B, Gao X, Li T Q, Hu Z M, Yu H M, Huang L. Structure confined porous Mo_2C for efficient hydrogen evolution[J]. Adv. Funct. Mater., 2017, 27(45): 1703933.

[46] Ma H B, Chen Z W, Wang Z L, Singh C V, Jiang Q. Interface engineering of Co/CoMoN/NF heterostructures for high-performance electrochemical overall water splitting[J]. Adv. Sci., 2022, 9(11): 2105313.

[47] Wang L, Fan J Y, Liu Y, Chen M Y, Lin Y, Bi H C, Liu B X, Shi N E, Xu D D, Bao J C, Han M. Phase-modulation of iron/nickel phosphides nanocrystals “armored” with porous P-doped carbon and anchored on P-doped graphene nanohybrids for enhanced overall water splitting[J]. Adv. Funct. Mater., 2021, 31(30): 2010912.

[48] Wang L, Fan J Y, Liu Y, Chen M Y, Lin Y, Bi H C, Liu B X, Shi N E, Xu D D, Bao J C, Han M. Phase-modulation of iron/nickel phosphides nanocrystals “armored” with porous P-doped carbon and anchored on P-doped graphene nanohybrids for enhanced overall water splitting[J]. Adv. Funct. Mater., 2021, 31(30): 2010912.

[49] Zhou X F, Tian Y H, Luo J, Jin B, Wu Z J, Ning X M, Zhan L, Fan X L, Zhou T, Zhang S Q, Zhou X S. MoC quantum dots@N-doped-carbon for low-cost and efficient hydrogen evolution reaction: From electrocatalysis to photocatalysis[J]. Adv. Funct. Mater., 2022: 2201518.

[50] Cai F F, Guo Y J, Ibrahim J J, Zhang J, Sun Y H. A highly active and stable Pd/MoC catalyst for hydrogen production from methanol decomposition[J]. Appl. Catal. B-Environ., 2021, 299: 120648.

焦耳热快速合成双功能电催化剂用于高效水分解

周 澳,郭伟健,王月青*,张进涛*

(山东大学化学与化工学院, 胶体与界面化学教育部重点实验室, 山东 济南 250100)

摘要: 电解水是有效的产氢方式之一, 开发具有高催化活性的电极材料是当前电解水的研究热点, 但仍面临诸多挑战。本研究报告了一种通过焦耳热技术快速制备多金属异质结构, 并将其用作电解水的双功能电催化剂, 展现出优异的电解水催化活性。通过焦耳热处理三种金属前驱涂覆的碳布, Mo_2C 和 CoO/Fe_3O_4 异质结构形成。当其用作析氢(HER)和析氧(OER)的双功能催化剂时, 仅需 121 mV 和 268 mV 的过电位,可以实现 10 mA·cm^{-2} 的电流密度。当用于两电极电解水时, MoC/FeO/CoO/CC 作为阳极和阴极催化剂表现出优异的电催化性能和长期稳定性, 仅需 1.69 V 即可实现 10 mA·cm^{-2} 的电流密度, 并且展现出 25 小时的稳定性。本研究通过简单、快速的焦耳热技术实现了双金属/多金属异质结构的构筑,并应用于高效水电解,为合理设计多金属异质结构提供指导。

关键词: 氢析出反应;氧析出反应;双功能电催化剂;水分解;焦耳热